Clays and Clay Minerals, Vol. 44, No. 5, 573–586, 1996.

REDOX CHARACTERIZATION OF THE SURFACES OF SEVEN IRON-BEARING MINERALS: USE OF MOLECULAR PROBES AND UV-VISIBLE SPECTROSCOPY

Y. SHANE YU[1,†] AND GEORGE W. BAILEY[2]

[1] Dyn-Corp Technology Applications, Inc., 960 College Station Road, Athens, Georgia 30605-2700

[2] Ecosystems Research Division, National Exposure Research Laboratory, U.S. Environmental Protection Agency, 960 College Station Road, Athens, Georgia 30605-2700

Abstract—Redox properties of iron-bearing mineral surfaces may play an important role in controlling the transport and transformation of pollutants into ground waters. Suspensions of seven iron-bearing minerals were reacted with pH and redox indicators under anaerobic conditions at the pH of the natural suspension. The responses of the indicators to the mineral surfaces were monitored by UV-visible spectroscopy using a scattered transmission technique. The Hammett surface acidity function (H_s) and the surface redox potential (Eh_s) of these iron-bearing minerals were measured. These measured values were used to calculate Eh values for the seven minerals: goethite = +293 mV; chlorite = +290 mV; hematite = +290 mV; almandite = +282 mV; ferruginous smectite = +275 mV; pyrite = +235 mV; and Na-vermiculite = +223 mV. Calculated surface redox potentials of minerals are different from their potentials measured by platinum electrode in bulk suspensions. UV-visible spectroscopy provides a quick and non-destructive way of monitoring organic probe response at the mineral surface.

Key Words—Electron activity, Indicators, Iron-bearing minerals, Redox potential, Surface acidity, UV-visible spectroscopy.

INTRODUCTION

Iron-bearing minerals are important constituents of soils, sediments and aquifer materials (Brown et al. 1978; Murad and Fischer 1988; Schwertmann and Taylor 1989). Anoxic zones occur both within the interstices of soil peds and within the 1 to 5 cm stratum below the water-sediment interface. These zones play an important role in controlling speciation and partitioning of both organic and inorganic pollutants between the aqueous and particulate phases and therefore, in controlling the transport and transformation of these pollutants in soil, sediment and groundwater.

The concept of employing molecular probes serving as indicators and UV-visible spectroscopy to investigate surface properties of mineral surfaces was proposed by Bailey and Karickhoff (1973) and Karickhoff and Bailey (1976). They investigated the interaction of various organic bases and basic pesticides with clay mineral surfaces, and monitored the protonation of these indicators of basic organic compounds at the mineral surfaces under varying water contents by UV-visible spectroscopy. UV-visible spectroscopy has several advantages over other methods (Bailey and Karickhoff 1973) in that: 1) it can measure protonation *in situ*, in suspension as well as films and slurries; and 2) it is very sensitive. Low levels of indicator loadings, for example <0.1% of cation exchange capacity for some indicator-mineral systems, can be quantitatively and reproducibly monitored. Cenens and Schoonheydt (1988) reported that methylene blue was a sensitive fingerprint molecule for probing the surface properties of clays within an aqueous suspension using UV-visible spectroscopy.

The redox potential of a chemical solution has been characterized as an important variable for chemistry since the 1920s (Conant 1926; Zobell 1946; Hewitt 1950; Bates 1959; Clark 1960; Guenther 1975). Many studies (Ponnamperuma et al. 1967, Ponnamperuma 1972; Loughnan 1969; Liu 1985; Bartlett 1986; Lindsay 1988) have reported the critical role for redox potential within natural environments such as soils or water/sediment systems. Conventional redox measurements have been made in the presence of solid phases, but the role of electron donors/acceptors on surfaces has not been delineated. Platinum electrodes were also used to measure the redox potential of porous media, but have known limitations (Ponnamperuma 1972; Bohn et al. 1979; Liu 1985; Stumm and Morgan 1985). Therefore, a reproducible *in situ* method is needed to characterize and estimate the redox potential at the interfacial region of mineral suspensions.

The surface acidity and the redox potential of iron-bearing minerals are critical parameters for understanding redox chemistry of soils or sediment systems (Ponnamperuma 1972; Bohn et al. 1979; Liu 1985; Stumm and Morgan 1985). Since details of the generalized surface acidity function and surface redox potential are of major importance in this study, equations

† Current address: Equifax, Inc., Decision Systems, External Maildrop 425, 1525 Windward Concourse, Alpharetta, Georgia 30202.

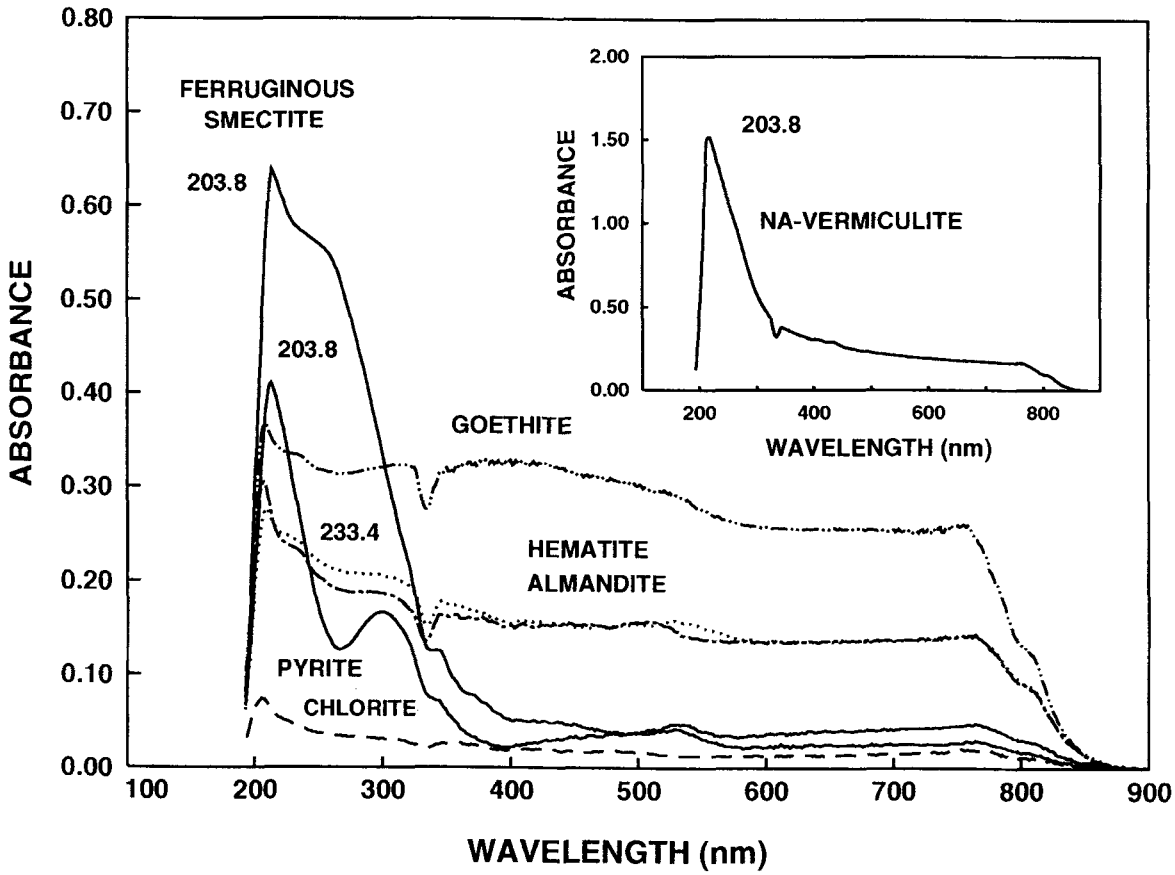

Figure 1. UV-visible spectra of 7 Fe-bearing mineral suspensions.

for these parameters are reviewed and described in the following sections.

Generalized Surface Acidity Function

The equation for the Hammett surface acidity, H_s, is:

$$H^+ \; Ind \overset{H_s^+}{\underset{K_a}{\leftrightarrow}} Ind_c \qquad [1]$$

and

$$pH_s = -\log K_a + \log\left(\frac{Ind}{Ind_c}\right) \qquad [2]$$

where Ind and Ind_c = the conjugate indicator species concentrations differing by one proton; K_a = the acidity constant describing the equilibrium between the two indicator species under ideal aqueous solution behavior; and s = the surface phase.

Generalized Oxidation-Reduction Reaction

The fundamental oxidation-reduction reaction at equilibrium can be expressed as:

$$Oxidant + n\ e^- \leftrightarrow Reductant \qquad [3]$$

The quantitative relationship between Eh and an electron donor and acceptor within solution is given by the classical Nernst equation:

$$E_{aq} = E^\circ + \left(\frac{RT}{nF}\right)\ln\left(\frac{\text{electron acceptor}}{\text{electron donor}}\right) \qquad [4]$$

at 25 °C

$$Eh_{aq} = E^\circ + \left(\frac{0.059}{n}\right)\log\left(\frac{\text{oxidized form}}{\text{reduced form}}\right) \qquad [5]$$

where Eh_{aq} = solution phase redox potential, mV; E° = standard potential, mV; T = temperature, °K; R = molar gas constant; F = Faraday's constant; and n = stoichiometric coefficient.

E° is the standard potential representing the capability of a redox couple to donate or accept electrons under standard conditions. For a given couple, the ratio of electron acceptor to electron donor is the ratio of its oxidized form concentration divided by its reduced form concentration. Therefore, if the oxidized-reduced/concentration ratio, and if the standard potential and the pH are known, it is possible to calculate Eh *a priori.*

https://doi.org/10.1346/CCMN.1996.0440501 Published online by Cambridge University Press

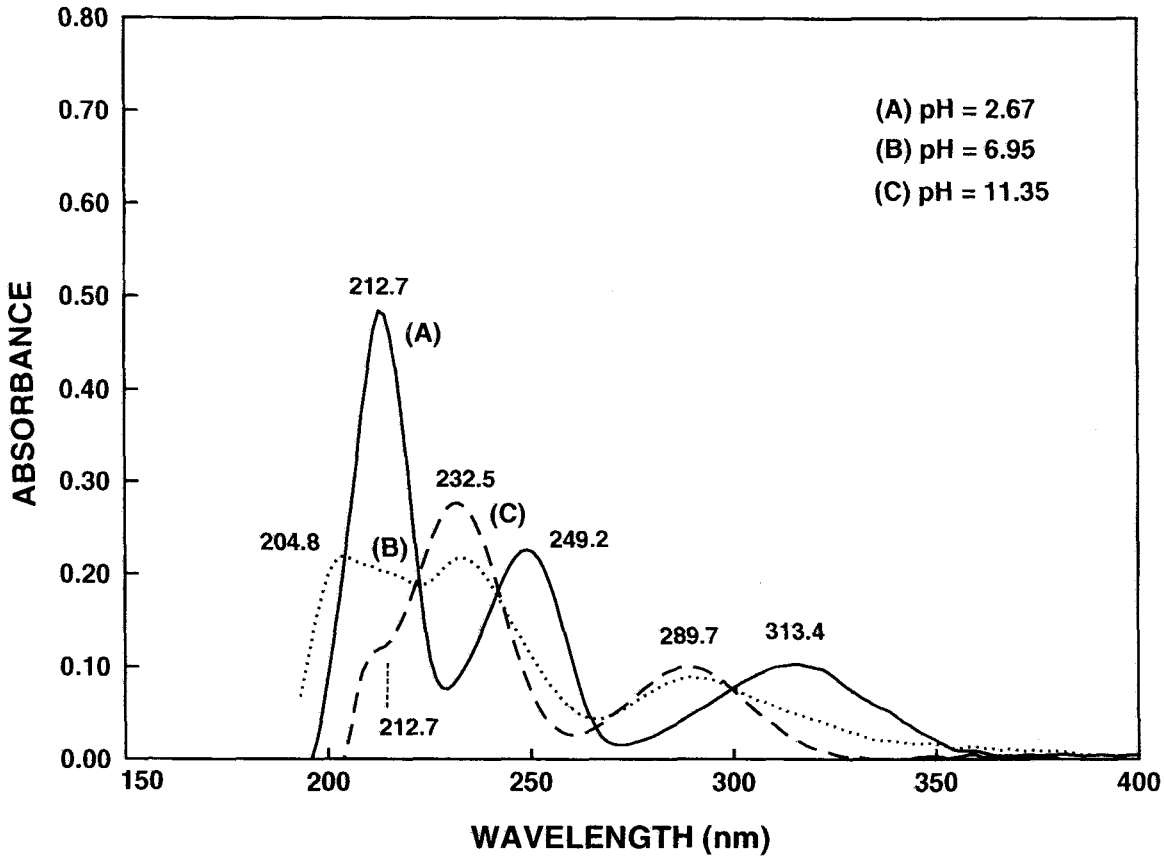

Figure 2. UV spectra of 3-aminopyridine at pH 2.67, 6.95 and 11.35.

Generalized Surface Redox Potential

The surface redox potential, Eh_s, of a porous medium reflects the steady state condition. Generally, porous media approach equilibrium very slowly, if at all. This appears to be true for the various redox systems in soils and sediments, for example, O, S, N, Fe, Mn and the C species. Speciation of a metal ion within the pore water governs its mobility and bioavailability. Metal ion speciation is governed by pH and electron activity (quantity of electrons within the system) where speciation reflects the ion oxidation number. The negative log a_e, where a_e is electron activity, is given by the analogous relationship to pH, $p_e = -\log a_e$. Reduction reactions are generally accompanied by the participation of protons. The general reaction can be written as:

$$\text{(Reductant = electron donor)} \leftrightarrow \text{(oxidant = electron acceptor)} + ne^- + mH^+ \quad [6]$$

where m = the stoichiometric coefficient of the hydrogen ion.

Eh_s is related to pH_s by the following relationship (Ponnamperuma 1972; Bohn et al. 1979; Liu 1985):

$$Eh_s = E^\circ + \frac{0.059}{n} + \log\frac{\text{Oxidant}}{\text{Reductant}} - 0.059\ (m/n)\ pH_s \quad [7]$$

Therefore, an estimate of surface redox potential can be made using a bracketed series of redox and acid-base probes, generalized surface reactions and the Hammett surface acidity (pH_s). Proton activity at or near a surface is not represented by bulk pH measurements. Similarly, it may be expected that the electron activity at or near a surface such as an iron-bearing mineral surface may not be represented by bulk phase redox potential measurements.

A method sensitive to both surface proton activity and surface electron activity is required to describe both the electron and proton reactivity at a mineral surface. Organic molecules whose protonated and unprotonated forms (acidity), oxidized and reduced forms (redox capacity) can serve as such monitors if these forms are spectroscopically different (Bailey and Karickhoff 1973). Bailey and Karickhoff's method

https://doi.org/10.1346/CCMN.1996.0440501 Published online by Cambridge University Press

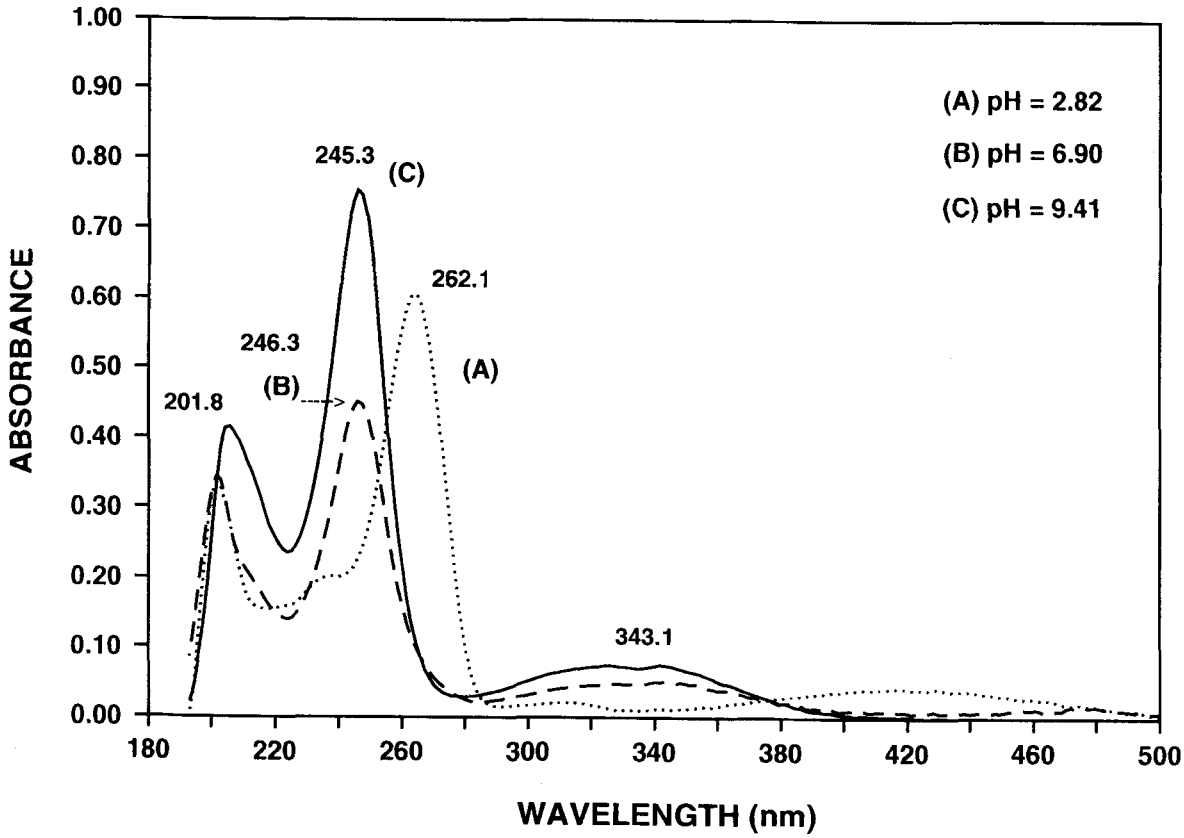

Figure 3. UV spectra of 5-aminoquinoline at pH 2.82, 6.90 and 9.41.

employed a UV-visible method for monitoring the surface acidity of clay minerals. They reported that this method could measure protonation *in situ* under wet or dry conditions and was very sensitive. They also reported that low levels of indicator loadings were quantitatively and reproducibly measured without interfering with the systems measured. Another advantage was that certain organic molecules showed sufficient changes within their optical spectra that one could distinguish between the adsorbed and unadsorbed species within the presence of a surface reaction.

We build upon their method by investigating the redox properties of seven minerals using both redox indicators and pH indicators as molecular probes. UV-visible spectroscopy was employed to study varying concentrations of mineral-water mixtures. Hammett acidity and estimated surface redox potential of these mineral suspensions were also determined. Batch-type experiments using both suspensions and solid films of minerals were conducted at 25 °C under anaerobic conditions and the indicator changes were monitored by UV-visible spectroscopy.

MATERIALS AND METHODS

Starting Materials

Indicators of redox (2,6-dichloroindophenol) and pH (5-aminoquinoline, and 3-aminopyridine) were obtained from Aldrich Chemical Company‡ and were used without further purification. Goethite (El Paso County, TX), hematite (Ishpenming, MI), almandite (Warren County, NY), pyrite (Huanzala, Peru) and chlorite (Ishpenming, MI) were obtained from Ward's Scientific Establishment. Na-vermiculite (Llano, TX) and ferruginous smectite (Grant County, WA) were obtained from the Clay Minerals Society. Each mineral sample was crushed using a shatter box (Spex Industries, Inc.) for 2 min, then screened using a nested series of sieves (0.131 mm, 0.091 mm, 0.064 mm, and 0.044 mm wire diameters). Immediately after the size reduction operations, the smallest fraction, which was smaller than 0.044 mm, was stored in a nitrogen-purged container. The mineral suspensions which were less than 2 μm in diameter were prepared using the

‡ Mention of commercial products does not constitute any endorsement by the U.S. Environmental Protection Agency.

https://doi.org/10.1346/CCMN.1996.0440501 Published online by Cambridge University Press

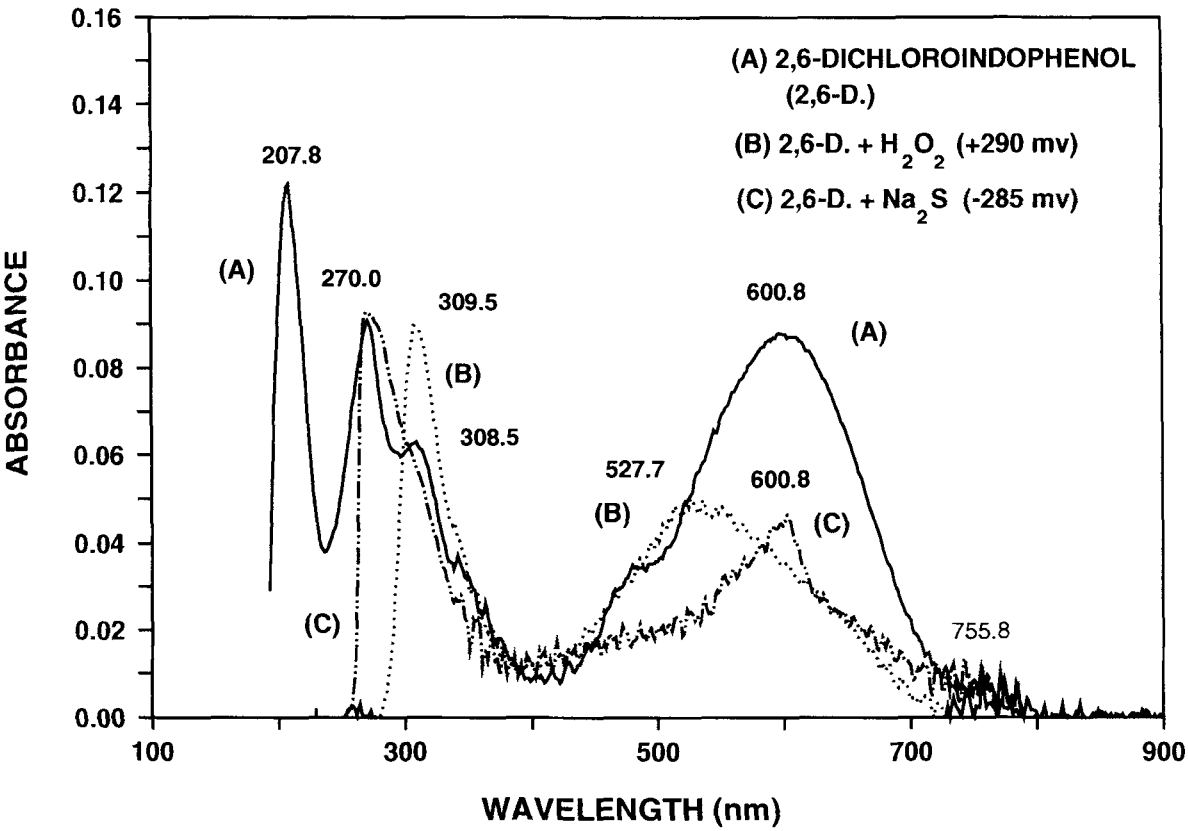

Figure 4. UV-visible spectra of 2,6-dichloroindophenol reacted with hydrogen peroxide and sodium sulfide.

Stoke's Law settling method (Jackson 1956). The raw mineral sample was mixed with boiled water previously purged with nitrogen (99.999%) for 10 min in a 100-ml cylinder capped tightly with a rubber sleeve. The cylinder was shaken for 1 min and the contents were allowed to settle. At selected time intervals, according to Stoke's Law, the suspension containing a particle size distribution of less than 2 μm was transferred into a flask using a rubber sleeve and purged with nitrogen for 10 min to remove dissolved CO_2 and O_2.

Criteria of Selecting Indicators

Selecting appropriate acid-base or redox indicators was an important step for this study. Six criteria were considered: 1) the indicator for either acid/base or oxidized/reduced forms had to be spectroscopically distinguishable and have a high molar absorptivity; 2) the redox indicator had to have an appropriate E° range and the acidity indicator had to have an appropriate acidity span; 3) the solubility of the indicator had to be high; 4) the indicator must not be capable of participating in other reactions that would interfere with the monitoring; 5) the indicator must have minimal toxicity; and 6) the indicator should not be light sensitive. The ideal indicator was not easy to find, and compromise was necessary based on the unique characteristics of a given system.

pH and Eh Measurement

A weighed amount of dried iron-bearing mineral suspended in boiled and degassed water was transferred to a sealed container that had designated access locations for electrode installation for pH and Eh measurements. The container was purged with dry, pure nitrogen. Measurements of pH and Eh were obtained with an Orion E940 expandable ion analyzer. The instrument was equipped with a Fisher Pt wire electrode and an Orion double junction reference electrode for Eh measurement, and with a Corning semi-micro pH combination electrode for pH measurement. The redox standard solution was prepared according to Light's procedure (1972) and contained 0.1 *M* ferrous ammonium sulfate, 0.1 *M* ferric ammonium sulfate and 1.0 *M* H_2SO_4. After each Eh measurement, the Pt electrode was rinsed 6 times with deionized water and cleaned with paper wipes. The Pt electrode was routinely cleaned by immersion into 0.06 *M* HCl solution, followed by washing with deionized water.

UV-visible Spectra

The preparation of mineral suspensions with concentrations ranging from 1.024 to 1.034 mg/ml under

https://doi.org/10.1346/CCMN.1996.0440501 Published online by Cambridge University Press

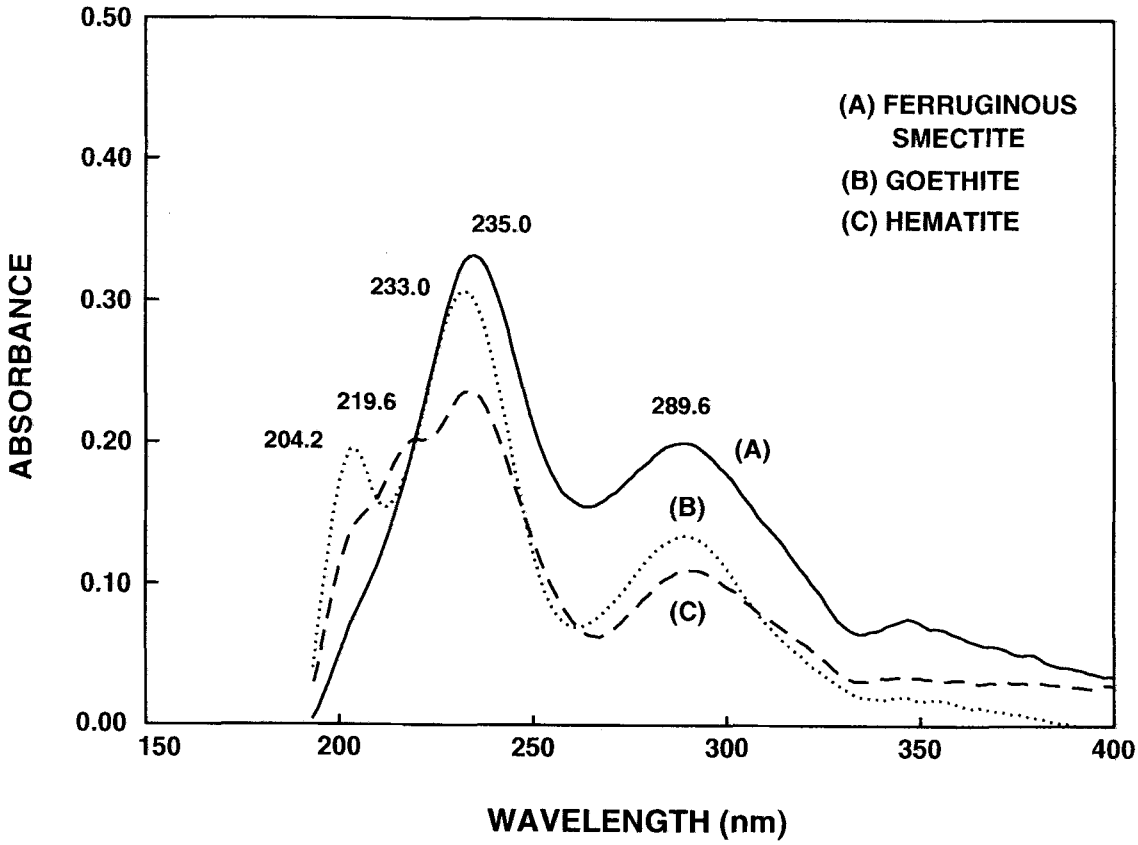

Figure 5. UV spectra of 3-aminopyridine reacted with ferruginous smectite, goethite and hematite.

anaerobic conditions for UV-visible scans was similar to the method of Ljungdahl and Andreesen (1978). Each mineral suspension was prepared by mixing the mineral sample with boiled-nitrogen-purged deionized water. Transferring the water and suspension to a closed vessel was conducted by gas-tight syringes under purged nitrogen. A Perkin-Elmer Lambda 4C UV-visible spectrophotometer with a scattered transmission accessory was used to monitor the spectral changes of the molecular probe. This accessory reduced the influence of radiation scattering within the suspensions.

The photo multiplier was located next to the cell holder so that light scattering was minimized. A Perkin Elmer #7300 computer was used to control the spectrophotometer and collect spectral data. The spectrophotometer was calibrated by a holmium oxide glass filter prior to analysis. Background correction was also conducted routinely. Each sample was transferred by a gas-tight syringe into a Spectral Cell R-2010-I 1 × 1 × 4 cm^3 cuvette and capped with a highly elastic Teflon/silicone septum. A blank solution was prepared the same way except there was no indicator within the cuvette and the cuvette was placed into the reference cell position.

The final concentrations of indicators for the mineral suspensions were 3.3×10^{-5} *M* for 2,6-dichloroindophenol and 8.9×10^{-6} *M* for both 3-aminopyridine and 5-aminoquinoline. Spectroscopic absorptivities of the neutral and protonated forms and the oxidized and reduced forms of the indicators were determined both for water and mineral-containing suspensions. The spectrum observed was that an indicator within the iron-bearing mineral suspension. To maintain good mixing conditions during the UV-visible scanning, a magnetic stirrer was placed into the cuvette and controlled by a Hellma CUV-O-STIR model 333 device. After each scan, the cuvette was rinsed 6 times with deionized water to remove all traces of the sample material.

Iron-bearing Minerals-Indicator Films

The solid mineral-indicator films were prepared by pipetting 1 ml of suspension (1.024 mg/ml) into the quartz cuvette (1 × 1 × 4 cm^3) that contained 5 μl of the stock indicator solution. The cuvette was then placed horizontally in a desiccator containing drierite which was obtained from W.A. Hammond Drierite Company. The degassing procedure was conducted for 16 h under vacuum conditions. After drying, the in-

https://doi.org/10.1346/CCMN.1996.0440501 Published online by Cambridge University Press

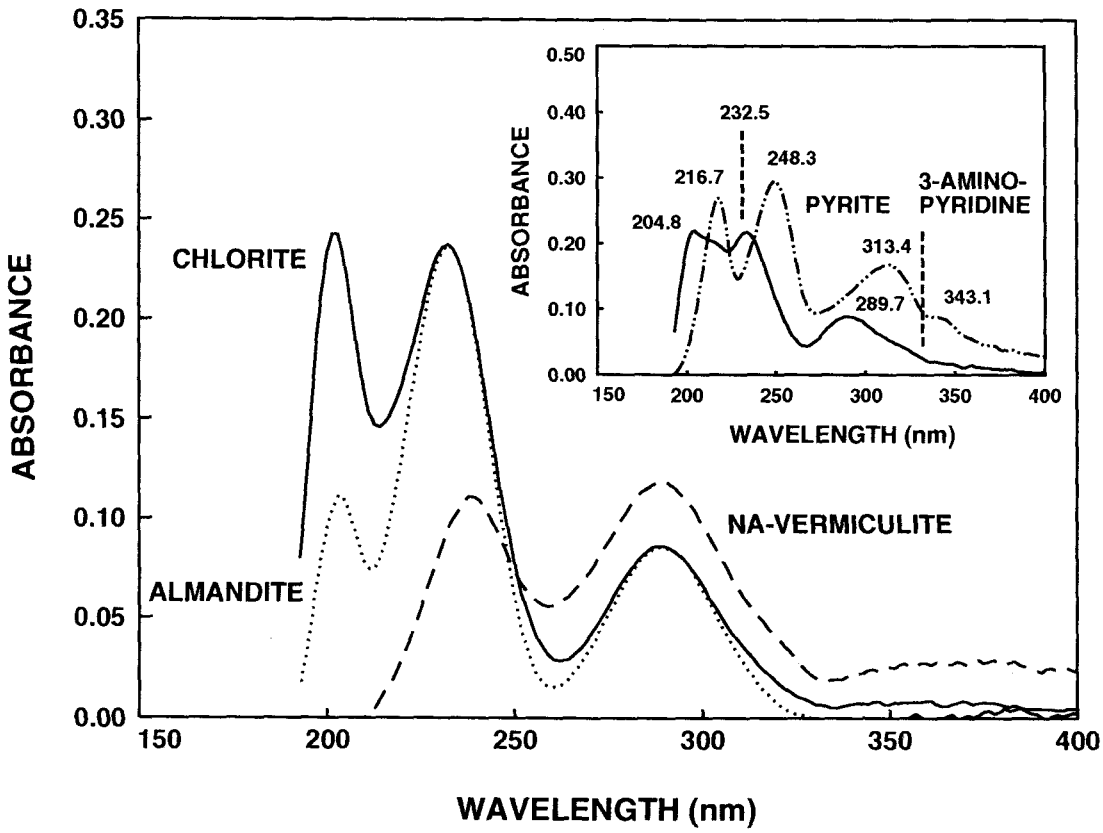

Figure 6. UV spectra of 3-aminopyridine reacted with almandite, chlorite, Na-vermiculite and pyrite.

dicator concentrations pipetted onto the film ranged from 2.21×10^{-8} to 3.83×10^{-8} moles/cm^2 for both redox and acid-base indicators. A blank Fe-bearing mineral film was prepared the same way except that no indicator was involved. A nitrogen (99.999%) purge was maintained while transferring the cuvette from the desiccator to the UV-visible spectrophotometer to minimize any contamination of surface acidity. Bailey and Karickhoff (1973) found that the presence of CO_2 influenced the final surface acidity value, so care was taken to exclude CO_2 as well as O_2.

RESULTS AND DISCUSSIONS

UV-visible Spectra of Seven Iron-bearing Minerals

The UV-visible spectra of the 7 iron-bearing minerals are shown in Figure 1. Each mineral suspension had a common peak at 203.8 nm. Goethite, hematite and almandite had a similar shoulder band at 233.4 nm. Pyrite had a unique peak at 300.0 nm, which the 6 other minerals did not have. There was a spectrum discontinuity at 223.5 nm, which was an instrumental signal generated due to the large amount of solid par-

Table 1. Redox and acidity characterization of 7 Fe-bearing mineral suspensions.

	Almandite	Chlorite	Ferruginous Smectite	Goethite	Hematite	Na-Vermiculite	Pyrite
Bulk pH	9.29	6.89	7.08	6.75	7.67	8.26	3.59
†Hammett Acidity	6.35	6.04	5.73	5.86	5.96	7.60	5.99
‡Hammett Acidity	6.53	6.24	6.41	6.15	6.33	7.37	5.89
pH Deviation	2.76	0.65	0.67	0.60	1.34	0.89	−2.30
Bulk Eh	129	237	235	208	166	188	362
§Surface Eh (mV)	282	292	275	293	290	223	235
Eh (mV) Deviation	−153	−55	−40	−85	−124	−35	127

† 3-aminopyridine was the molecular probe.
‡ 5-aminoquinoline was the molecular probe.
§ 3-aminopyridine and 2,6-dichloroindophenol were the molecular probes.

https://doi.org/10.1346/CCMN.1996.0440501 Published online by Cambridge University Press

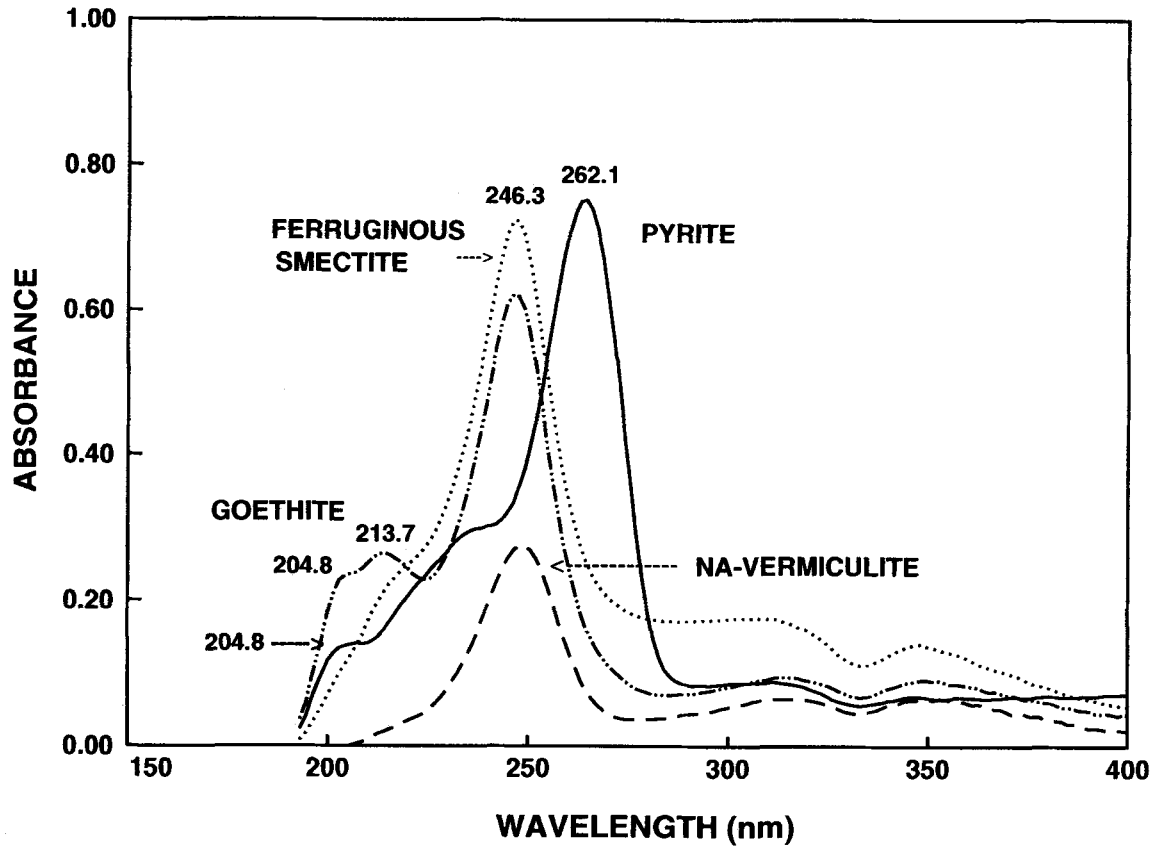

Figure 7. UV spectra of 5-aminoquinoline reacted with goethite, ferruginous smectite, pyrite and Na-vermiculite.

ticles within the suspension. A plateau that started at about 770.0 nm and ranged to 400.0 nm was due to the amount of solids within the suspension. Schwertmann (1971) found indications that hematite could frequently transform to goethite; therefore, it was not surprising to observe that both minerals had similar UV-visible spectra.

Characterization of the Acid-Base Indicators

To characterize the property of indicators, a series of experiments was conducted to monitor the response range of either an acid-base indicator or a redox indicator. Exploring the response range of acid-base indicators for varying pH environments was essential because the response range was an indication of how effectively the indicators could perform within a given pH system. Figure 2 shows the UV-visible spectra of 3-aminopyridine, pK_a = 6.03 at 3 different pH conditions. This shows that a given system could be monitored at 248.3 nm. The protonation of 3-aminopyridine has been proposed from organic chemistry studies (Perrin et al. 1981), and the detailed speciation is illustrated in Equation [8].

ACID-BASE INDICATORS

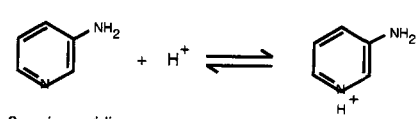

3-aminopyridine

(pKa = 6.03) [8]

Figure 3 shows the UV-visible spectra of 5-aminoquinoline, pK_a = 5.42, in acidic, neutral and basic environments. A unique peak at 262.1 nm was observed when 5-aminoquinoline was exposed to a more acidic environment, pH 2.82. The protonation of 5-aminoquinoline is illustrated in Equation [9].

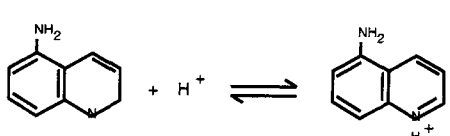

5-aminoquinoline

(pKa = 5.42) [9]

https://doi.org/10.1346/CCMN.1996.0440501 Published online by Cambridge University Press

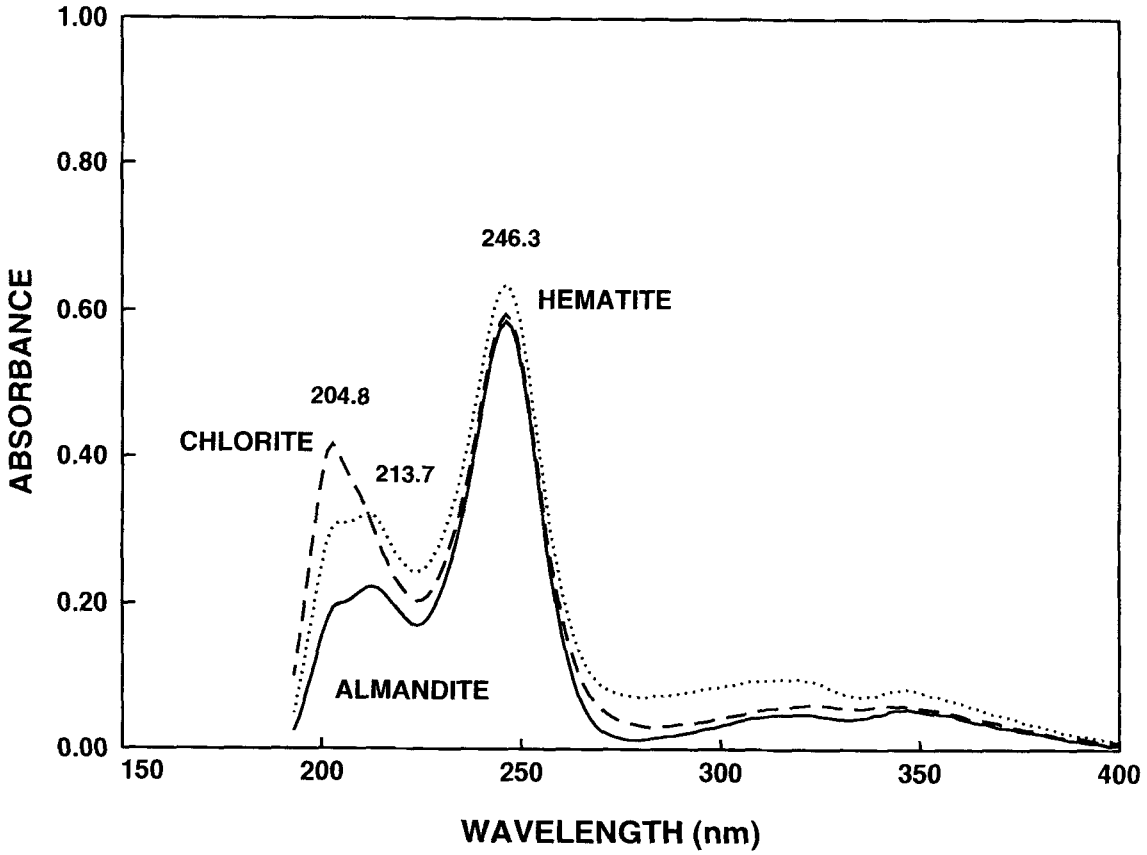

Figure 8. UV spectra of 5-aminoquinoline reacted with almandite, chlorite and hematite.

Characterization of the Redox Indicator

The response range of 2,6-dichloroindophenol within varying redox conditions was also crucial for our molecular probe system. Figure 4 shows the UV-visible spectra of 2,6-dichloroindophenol reacted with a typical oxidizing agent, H_2O_2, and a typical reducing agent, Na_2S. Figure 4 also indicates that, for a moderately oxidizing environment (such as H_2O_2, +290 mV), the 600.8 nm band shifts to 527.7 nm which is perhaps due to complexation or to protonation. There was no significant peak at 600.8 nm. Under reduced conditions such as Na_2S, −285 mV, the absorbance of the 600.8 nm peak decreased, as predicted. Because there was only one peak at 600.8 nm that consistently responded to the electron activity in this system, a reference Eh value at pH = 7 with 50% for the reduced form and 50% of the oxidized form that is, 217 mV; (Hewitt 1950) was required. Absorbance of measured systems were monitored at 600.8 nm. The initial color of 2,6-dichloroindophenol solution was blue. When it was put into a reducing environment, the blue disappeared and the solution became colorless. Mechanisms of the shifting from blue to red or from blue to colorless are illustrated in Equation [10].

REDOX INDICATOR

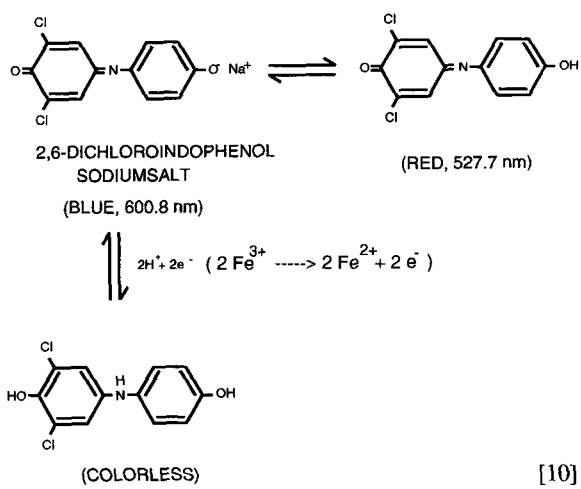

[10]

Probing the Surface Acidity of Iron-bearing Minerals

The UV-visible spectra of 3-aminopyridine reacting with ferruginous smectite, goethite and hematite is

https://doi.org/10.1346/CCMN.1996.0440501 Published online by Cambridge University Press

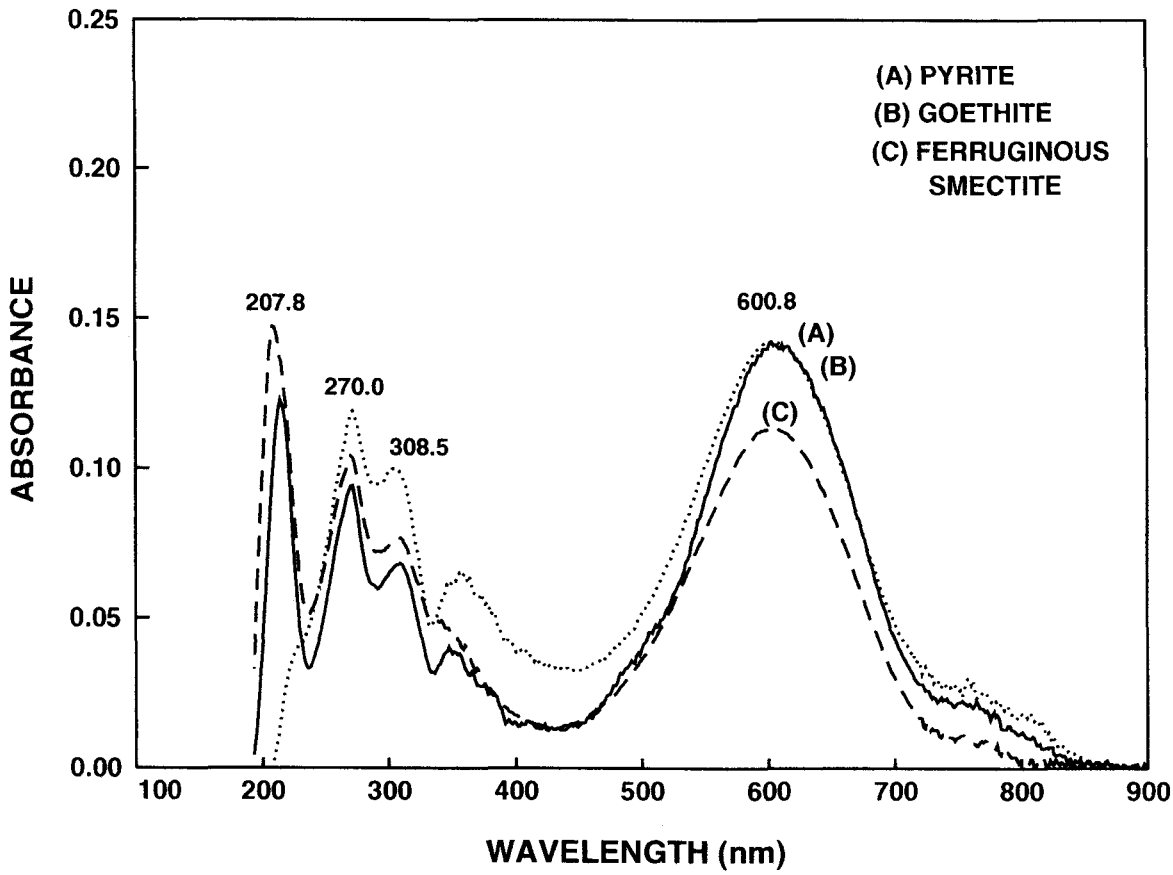

Figure 9. UV-visible spectra of 2,6-dichloroindophenol reacted with goethite, ferruginous smectite and pyrite.

shown in Figure 5. The Ind/Ind_c term in Equation [2] was calculated as the absorbance at 219.6 nm divided by the absorbance at 233.0 nm for goethite and hematite and the absorbance at 219.6 nm divided by the absorbance at 235.0 nm for ferruginous smectite. Similarly, Ind/Ind_c was calculated as the absorbance ratio of 204.2 nm versus 233.0 nm for almandite and chlorite, and 204.2 nm versus 242.0 nm for Na-vermiculite (Figure 6). Pyrite had a unique absorbance ratio of 216.7 nm versus 248.3 nm. The calculated Hammett surface acidity is summarized in Table 1.

Comparing Figure 2 to Figures 5 and 6, for example, the UV-visible spectra of free molecules in solution and adsorbed species on the mineral surface, we found that the wavelength of the monitored peak of the adsorbed species shifted from 2 to 18 nm.

The UV-visible spectra of 5-aminoquinoline reacted with seven mineral suspensions are shown in Figures 7 and 8. The term Ind/Ind_c was calculated as the absorbance at 246.3 nm divided by the absorbance at 262.1 nm. The calculated results are given in Table 1.

Probing the Surface Redox Potential of Iron-bearing Minerals

From Equation [7] it was noticed that the term "0.059 (m/n) pH" had greater impact than the term "log(Oxd/Red)" on Eh_s. Particularly for the UV-visible spectra (Figures 9 and 10), the absorbance differences at 600.8 nm among the 7 iron-bearing mineral suspensions were not very large. Therefore, after taking the logarithm of the Oxd/Red quotient, the impact was not as significant as the role of "0.059 (m/n) pH". When m = n = 1, every increment of pH could increase Eh by 59 mV. For goethite and the hematite systems, with the redox reaction at equilibrium, that is:

$$FeOOH_{(s)} + 3H^+ + e^- \leftrightarrow Fe^{2+}{}_{(aq)} + 2\ H_2O \quad [11]$$

the quotient of m/n was 3. Thus, the impact of surface acidity on Eh_s could be great.

Interpreting the redox potential was not easy, due to the complexity of the mineral suspension systems. Three key assumptions were necessary: 1) the heterogeneity of iron-bearing minerals was a minor factor; 2) equilibrium was established, that is, mineral dissolution was not considered; and 3) the m/n quotient was assumed to be 3 for the 6 iron-bearing minerals except pyrite.

The redox and acidity characterization results of the 7 iron-bearing minerals are summarized in Table 1,

https://doi.org/10.1346/CCMN.1996.0440501 Published online by Cambridge University Press

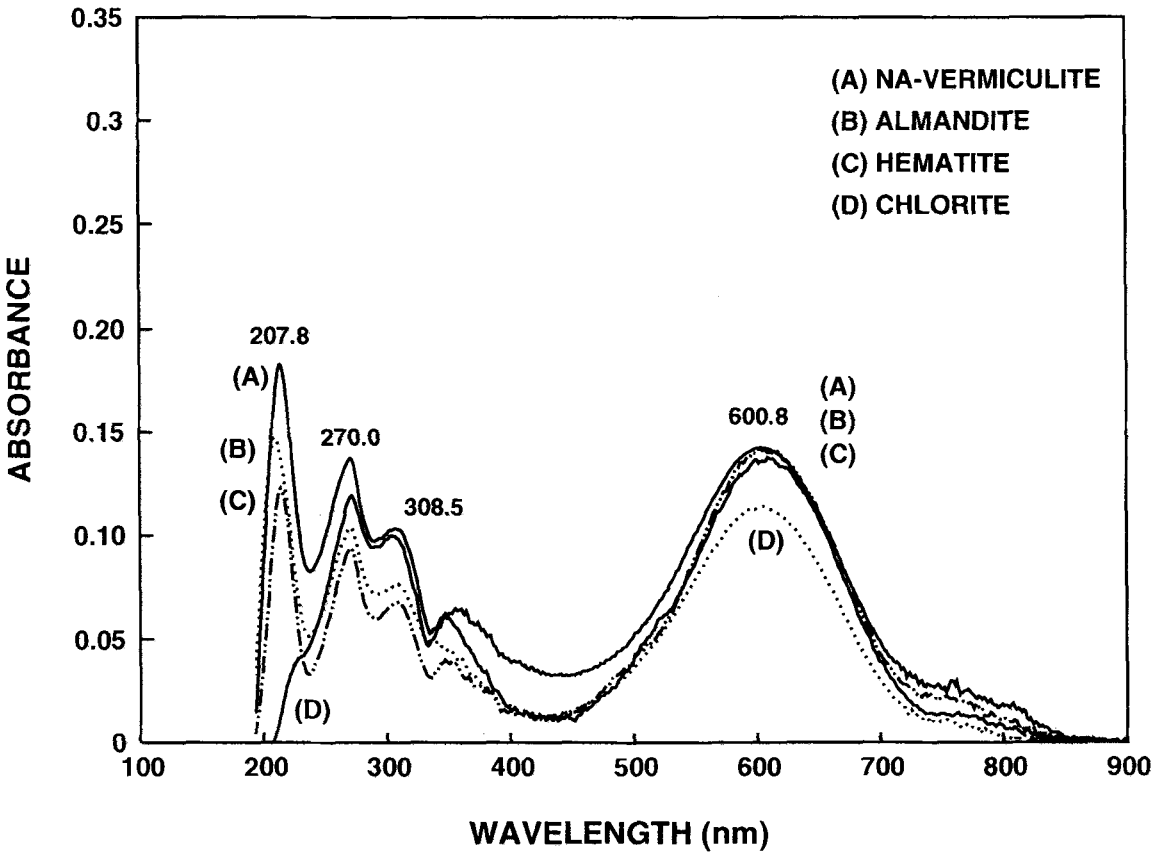

Figure 10. UV-visible spectra of 2,6-dichloroindophenol reacted with almandite, chlorite and Na-vermiculite.

where 3-aminopyridine and 2,6-dichloroindophenol were used to calculate the mineral Eh. The data show that the Hammett surface acidities for all minerals except pyrite were more acidic than the bulk pH values, which were measured by electrodes. Also the surface Eh values which were obtained using molecular probe indicators and UV-visible spectroscopy, reflected a more oxidized environment than the bulk Eh values for all minerals except pyrite. The relationship between Eh and pH for these 7 minerals is illustrated in Figure 11. This figure indicates that the bulk Eh-pH data are scattered over a larger range than the calculated surface Eh-pH values. For bulk Eh-pH values, an equation:

$$Eh_b\ (mV) = -40.40\ (pH_b) + 503 \qquad [12]$$

was determined by linear regression. For surface Eh-pH values, an equation:

$$Eh_s = -59.23\ (pH_s) + 661 \qquad [13]$$

was obtained. The surface Eh-pH values showed a slightly higher correlation coefficient ($R^2 = 0.96$) than the measured bulk values ($R^2 = 0.94$). Pyrite deviated from the regression line of the surface data more than other minerals. The reason could be that complex surface reactions occurred and labile species such as S^{2-}, SO_3^{2-}, SO_4^{2-}, $S_2O_3^{2-}$, $S_4O_6^{2-}$ and $S_nO_6^{2-}$ generated on the pyrite surface (Goldhaber 1983; Luther 1987; Moses et al. 1987).

UV-visible Spectra of Goethite Film

The UV-visible spectra of 5-aminoquinoline alone and reacted with a goethite suspension and with a goethite solid film, are shown in Figure 12. The adsorbed 5-aminoquinoline molecules on the goethite film showed a peak at 252.2 nm with a smaller absorbance rather than the goethite suspension (245.3 nm). These spectra also demonstrated that UV-visible spectroscopy was sensitive enough to monitor a low concentration such as 3.83×10^{-8} moles/cm^2 of indicator on a mineral film.

Proposed Mechanisms

For the equilibrium between an acid-base indicator and an iron-bearing mineral suspension, the following reactions are proposed:

https://doi.org/10.1346/CCMN.1996.0440501 Published online by Cambridge University Press

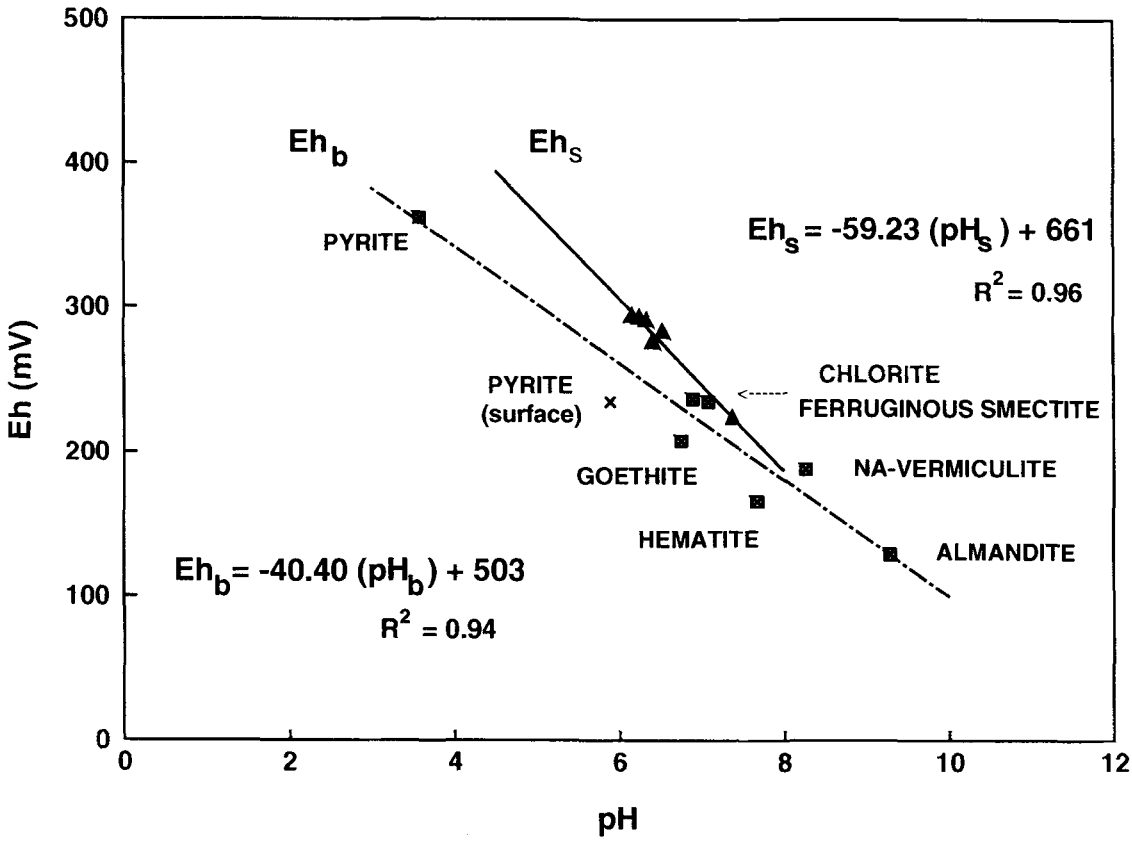

Figure 11. Relationship of pH_b-Eh_b and pH_s-Eh_s of 7 Fe-bearing minerals.

$$g(\equiv Fe\text{-}O^-)_s + H_2O \leftrightarrow a[Fe(H_2O)_6]^{3+}{}_{aq} + b(\equiv Fe\text{-}O^-)_s \quad [14]$$

$$a[Fe(H_2O)_6]^{3+}{}_{aq} \leftrightarrow a[Fe(OH)(H_2O)_5]^{2+}{}_{aq} + H_3O^+ \quad [15]$$

$$H_3O^+ + (Ind)_{aq} \leftrightarrow (Ind\text{-}H^+)_{aq} \quad [16]$$

$$b(\equiv Fe\text{-}O^-)_s + H_2O \leftrightarrow b(\equiv Fe\text{-}OH)_s + OH^-{}_{aq} \quad [17]$$

$$b(\equiv Fe\text{-}OH)_s + (Ind)_{aq} \leftrightarrow b(\equiv Fe\text{-}OH \cdot Ind^+)_s \quad [18]$$

where g, a, b = stoichiometry of the Fe mineral at equilibrium; s = solid phase; aq = solution phase; Ind = acid base indicator, 3-aminopyridine or 5-aminoquinoline; Ind-$H^+{}_{aq}$ = protonated acid-base indicator within solution equilibrium; and $\equiv$Fe-OH-$Ind^+{}_s$ = acid-base indicator at the mineral surface.

The $\equiv$FeOH-$Ind^+{}_s$ acid-base complex should form on the crystal edges of the 3 phyllosilicates—chlorite, Na-vermiculite and ferruginous smectite. The other 4 minerals: almandite, goethite, hematite and pyrite, should bind the acid-base indicator on appropriate crystallographic faces.

Equations [14], [15] and [17] describe an Fe-bearing mineral at equilibrium between 2 phases, the mineral surface phase and the solution phase. Different Fe-bearing minerals may have various a and b values. Equation [16] describes the response of the acid-base indicator (3-aminopyridine or 5-aminoquinoline) within solution. (Ind-$H^+)_{aq}$ also describes the degree of protonation of the acid-base indicator within solution. The UV-visible spectroscopy using a scattered transmission accessory actually represents the molecular probe response of both mineral solution and surface phases that is, suspension.

Similarly, to illustrate the interactions between iron-bearing minerals and the redox indicator, 2,6-dichloroindophenol, the following reactions are proposed:

$$g(\equiv Fe\text{-}O^-)_s + H_2O \leftrightarrow a[Fe(H_2O)_6]^{3+}{}_{aq} + b(\equiv Fe\text{-}O^-)_s \quad [19]$$

$$a[Fe(H_2O)_6]^{3+}{}_{aq} \leftrightarrow a[Fe(OH)(H_2O)_5]^{2+}{}_{aq} + H_3O^+ \quad [20]$$

$$H_3O^+ + 2e^- + (Ind\text{-}O^-)_{aq} \leftrightarrow (Ind\text{-}OH)_{aq} \quad [21]$$

$$b(\equiv Fe\text{-}O^-)_s + H_2O \leftrightarrow b(\equiv Fe\text{-}OH)_s + OH^-{}_{aq} \quad [22]$$

https://doi.org/10.1346/CCMN.1996.0440501 Published online by Cambridge University Press

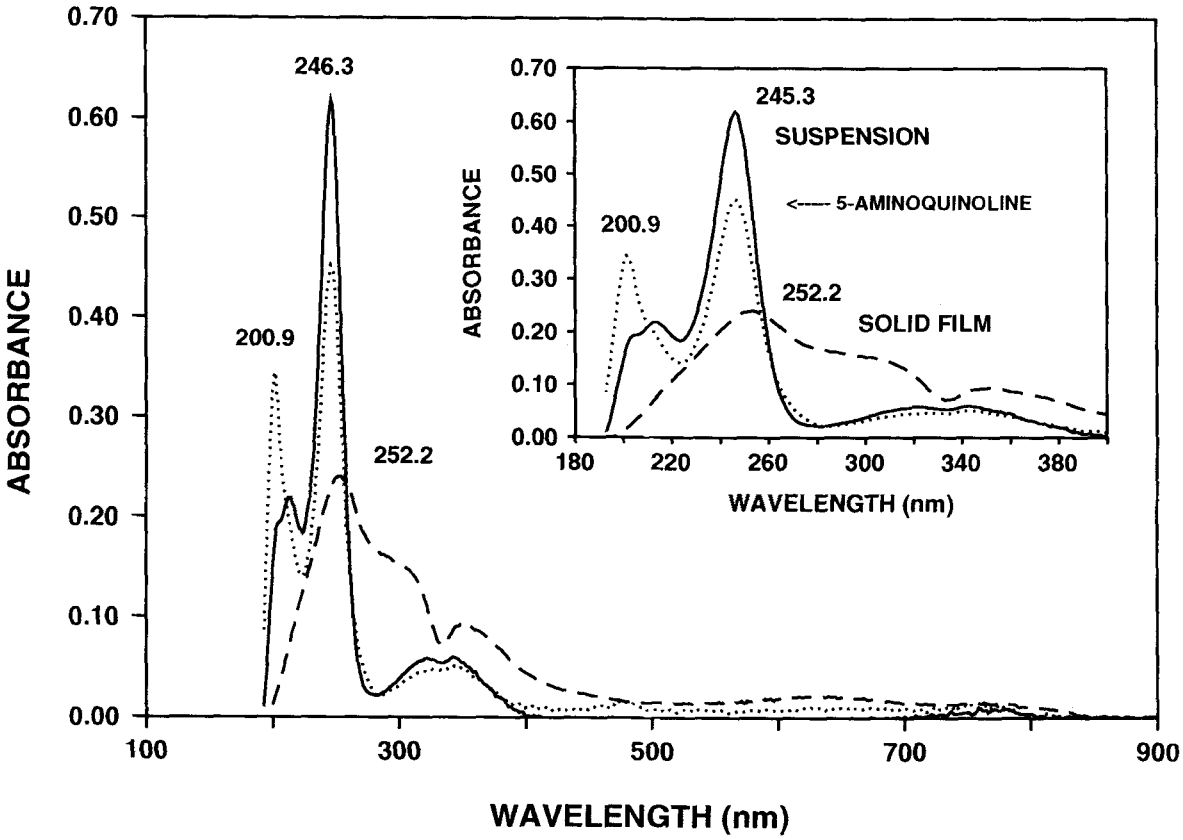

Figure 12. UV-visible spectra of 5-aminoquinoline reacted with goethite suspension and solid film.

$$b(\equiv Fe\text{-}O^-)_s + 2H^+ + 2e^- + b(Ind\text{-}O^-)_{aq} \leftrightarrow b(\equiv Fe\text{-}OH \cdot Ind\text{-}OH)_s \quad [23]$$

where g, a, and b = stoichiometry of the Fe mineral equilibrium; s = solid phase; aq = solution phase; $(Ind\text{-}O^-)_{aq}$ = 2,6-dichloroindophenol within solution (water); $(Ind\text{-}OH)_{aq}$ = 2,6-dichloroindophenol response to electron activity in water; and $(\equiv Fe\text{-}OH\cdot Ind\text{-}OH)_s$ = 2,6-dichloroindophenol response to electron activity at the Fe mineral surface.

Equation [23] is the response of the redox indicator at the interfacial region.

The bulk Eh obtained from the Eh electrodes measurement only represents the solution phase electron activity, that is the $(Ind\text{-}OH)_{aq}$. In the case of molecular probe approach, Eh_{aq} represents both the response $(Ind\text{-}OH)_{aq}$ within solution and the response $(\equiv Fe\text{-}OH\cdot Ind\text{-}OH)_s$ at the surface of the Fe-bearing mineral. Equation [19] is a generalized form for Fe-bearing minerals equilibrium. Each Fe-bearing mineral suspension may have different stoichiometry, and the deviations are taken into consideration with various a, b and g values.

CONCLUSIONS

Organic compounds such as 2,6-dichloroindophenol, 3-aminopyridine and 5-aminoquinoline can be used as molecular probes to evaluate the redox properties of iron-bearing minerals. The surface redox potentials, Eh_s, of iron-bearing minerals show slightly reducing conditions according to a general Eh scale (Patrick 1980; Wolfe et al. 1990). The organic molecules respond to the interfacial electron and proton activity and can be detected by UV-visible spectroscopy. Using a molecular probe approach, we found that, except for pyrite, the Hammett surface acidities of iron-bearing minerals were more acidic than the bulk pH values. Estimated surface Eh values were higher than the measured bulk Eh values, except for pyrite. The complexity or the ease with which oxidation occurred on a pyrite surface may contribute to the deviation. Experimental results indicate that surface redox properties are not equivalent to the redox properties of bulk or solution phases. UV-visible spectroscopy can be used to monitor surface redox reactions of varying mineral-water mixtures and is sensitive over a broad range including low indicator concentrations within suspension and on a dry film. This technique, com-

https://doi.org/10.1346/CCMN.1996.0440501 Published online by Cambridge University Press

bined with a scattered transmission accessory, can perform *in situ* measurements quickly, and does not change the characteristics of the sample. Investigating surface acidity and surface redox potential of these Fe-bearing minerals may aid in elucidating their roles in controlling the transport and transformation of pollutants within natural environments.

ACKNOWLEDGMENT

This research was supported in part through U.S. Environmental Protection Agency Contract No. 68-C1-0024 to DynCorp-Technology Applications, Inc.

REFERENCES

Bailey GW, Karickhoff SW. 1973. An ultraviolet spectroscopic method for monitoring surface acidity of clay minerals under varying water content. Clays Clay Miner 21: 471–477.

Bartlett RJ. 1986. Soil redox behavior. In: Sparks DL, editor. Soil physical chemistry. Boca Raton, FL: CRC Press. p 179–207.

Bates RG. 1959. Electrode potentials: Treatise on analytical chemistry, Part 1. In: Kolthoff IM, Elving PJ, editors. New York: Interscience. p 319–359.

Bohn HL, McNeal BL, O'Connor GA. 1979. Soil chemistry. New York: John Wiley and Sons. p 247–271.

Brown G, Newman ACD, Rayner JH, Weir AH. 1978. The structures and chemistry of soil clay minerals. In: Greenland DJ, Hayes MHB, editors. The chemistry of soil constituents. New York: John Wiley and Sons. p 29–178.

Cenens J, Schoonheydt RA. 1988. Visible spectroscopy of methylene blue on hectorite, laponite B, and barasym in aqueous suspension. Clays Clay Miner 36:214–224.

Clark WM. 1960. Oxidation-reduction potentials of organic systems. Baltimore, MD: Williams and Wilkins. p 1–106.

Conant JB. 1926. The electrochemical formulation of the irreversible reduction and oxidation of organic compounds. Chem Rev 3:1–40.

Goldhaber MB. 1983. Experimental study of metastable sulfur oxyanion formation during pyrite oxidation. Am J Sci 283:193–217.

Guenther WB. 1975. Chemical equilibrium. New York: Plenum Press. p 207–228.

Hewitt LF. 1950. Oxidation-reduction potentials in bacteriology and biochemistry. Edinburgh, UK: Livingstone. p 19–36.

Jackson ML. 1956. Soil chemical analysis—Advanced course. Published by the author, Dept. of Soils, Univ. of Wisconsin, Madison, WI. p 100–115.

Karickhoff SW, Bailey GW. 1976. Protonation of organic bases in clay-water systems. Clays Clay Miner 24:170–176.

Light TS. 1972. Standard solution for redox potential measurements. Anal Chem 44:1038–1039.

Lindsay W. 1988. Solubility and redox equilibria of iron compounds in soils. In: Stucki JW, Goodman BA, Schwertmann U, editors. Iron in soil and clay minerals. Norwell, MA: Kluwer Academic Publishers. p 37–61.

Liu Z. 1985. Oxidation-reduction potential. In: Yu T, editor. Physical chemistry of paddy soils. Beijing: Science Press. p 1–26.

Ljungdahl LG, Andreesen JR. 1978. Formate dehydrogenase, a selenium-tungsten enzyme from *Clostridium thermoaceticum*. Meth in Enzymol 53:360–372.

Loughnan FC. 1969. Chemical weathering of the silicate minerals. New York: American Elsevier. p 4–26.

Luther GW. 1987. Pyrite oxidation and reduction: Molecular orbital theory considerations. Geochim Cosmochim Acta 51:3193–3199.

Moses CO, Nordstrom DK, Herman JS, Mills AL. 1987. Aqueous pyrite oxidation by dissolved oxygen and by ferric iron. Geochim Cosmochim Acta 51:1561–1571.

Murad E, Fischer WR. 1988. The geobiochemical cycle of iron. In: Stucki JW, Goodman BA, Schwertmann U, editors. Iron in soils and clay minerals. Norwell, MA: Kluwer Academic Publishers. p 1–18.

Patrick WH, Jr. 1980. The role of inorganic redox systems in controlling reduction in paddy soils. In: Editor, China, Inst Soil Sci, Proc. Symposium on Paddy Soil. Nanjing, China: Academia Sinica. p 107–117.

Perrin DD, Dempsey B, Serjeant EP. 1981. Prediction of pKa for phenols, aromatic carboxylic acids and aromatic amines. In: Perrin DD, Dempsey B, Serjeant EP, editors. pKa prediction for organic acids and bases. Norwell, MA: Chapman and Hall. p 44–52.

Ponnamperuma FN, Tianco EM, Loy T. 1967. Redox equilibria in flooded soils. I. The iron hydroxide system. Soil Sci 103:374–382.

Ponnamperuma FN. 1972. The chemistry of submerged soils. In: Brady NC, editor. Advances in agronomy. New York: Academic Press. p 29–96.

Schwertmann U. 1971. Transformation of hematite to goethite in soils. Nature 232:624–625.

Schwertmann U, Taylor RM. 1989. Iron oxide. In: Dixon JB, Weed SB, editor. Minerals in soil environments. Madison, WI: Soil Sci Soc Am. p 379–438.

Stumm W, Morgan JJ. 1985. The conceptual significance of pe. A comment on J.D. Hostettler's paper, electrode electrons, aqueous electrons and redox potentials in natural waters. Am J Sci 285:856–859.

Wolfe NL, Mingelgrin U, Miller GC. 1990. Abiotic transformations in water, sediment, and soil. In: Cheng HH, editor. Pesticides in the soil environment: Processes, impact, and modeling. SSSA Book Series 2, Madison, WI: Soil Sci Soc Am. p 103–168.

Wurmser R, Banerjee R. 1964. Oxidation-reduction potentials. Compr Biochem 12:62–88.

Zobell CE. 1946. Studies on redox potential of marine sediments. Am Assoc Pet Geol Bull 30:477–513.

(Received 4 October 1994; accepted 30 August 1995; Ms. 2580)